

UC Irvine

UC Irvine Previously Published Works

Title

Response of the superparameterized Madden-Julian Oscillation to extreme climate and basic state variation challenges a moisture mode view

Permalink

<https://escholarship.org/uc/item/4xk1t6n6>

Journal

Journal of Climate, 29(13)

ISSN

0894-8755

Authors

Pritchard, Michael S
Yang, Da

Publication Date

2016-07-01

DOI

10.1175/jcli-d-15-0790.1

Peer reviewed

Response of the Superparameterized Madden–Julian Oscillation to Extreme Climate and Basic-State Variation Challenges a Moisture Mode View

MICHAEL S. PRITCHARD

Department of Earth System Sciences, University of California, Irvine, Irvine, California

DA YANG

*Department of Earth and Planetary Science, and Miller Institute for Basic Research in Science,
University of California, Berkeley, Berkeley, California*

(Manuscript received 5 November 2015, in final form 4 April 2016)

ABSTRACT

The climate sensitivity of the Madden–Julian oscillation (MJO) is measured across a broad range of temperatures (1°–35°C) using a convection-permitting global climate model with homogenous sea surface temperatures. An MJO-like signal is found to be resilient in all simulations. These results are used to investigate two ideas related to the modern “moisture mode” view of MJO dynamics. The first hypothesis is that the MJO has dynamics analogous to a form of radiative convective self-aggregation in which longwave energy maintenance mechanisms shut down for $SST \ll 25^\circ\text{C}$. Inconsistent with this hypothesis, the explicitly simulated MJO survives cooling and retains leading moist static energy (MSE) budget terms associated with longwave destabilization even at $SST < 10^\circ\text{C}$. Thus, if the MJO is a form of longwave-assisted self-aggregation, it is not one that is temperature critical, as is observed in some cases of radiative–convective equilibrium (RCE) self-aggregation. The second hypothesis is that the MJO is propagated by horizontal advection of column MSE. Inconsistent with this view, the simulated MJO survives reversal of meridional moisture gradients in the basic state and a striking role for horizontal MSE advection in its propagation energy budget cannot be detected. Rather, its eastward motion is balanced by vertical MSE advection reminiscent of gravity or Kelvin wave dynamics. These findings could suggest a tight relation between the MJO and classic equatorial waves, which would tend to challenge moisture mode views of MJO dynamics that assume horizontal moisture advection as the MJO’s propagator. The simulation suite provides new opportunities for testing predictions from MJO theory across a broad climate regime.

1. Introduction

The Madden–Julian oscillation (MJO) is a slow eastward-moving mode that is the most energetic intra-seasonal cycle in the tropical atmosphere. Although critical to regional weather and climate, its physics remain in debate (Zhang 2005; Raymond and Fuchs 2009; Majda and Stechmann 2009; Yang and Ingersoll 2013, 2014).

Until recently explicit MJO simulation has been difficult but new advances in modern multiscale atmospheric simulation (Grabowski and Smolarkiewicz 1999; Randall et al. 2003) have enabled realistic MJO simulation with minimal approximations (Khairoutdinov et al. 2005, 2008; Benedict and Randall 2009). Combined with new computational acceleration techniques (Pritchard et al. 2014; Jones et al. 2015), this technology now allows for ideas about MJO physics to be efficiently stress tested explicitly in extreme settings.

One idea worth exploring is the “moisture mode” view that the MJO is fundamentally energized and propagated by thermodynamic feedbacks acting to regulate the tropical

Supplemental information related to this paper is available at the Journals Online website: <http://dx.doi.org/10.1175/JCLI-D-15-0790.s1>.

Corresponding author address: Michael S. Pritchard, Assistant Professor, Department of Earth System Sciences, University of California, Irvine, 3200 Croul Hall, Irvine, CA 92697-3100.
E-mail: mspritch@uci.edu

Publisher’s Note: This article was revised on 28 June 2016 to fix a typographical error in the title.

moisture field (Raymond and Fuchs 2009; Sobel and Maloney 2012)—in turn a good proxy for the column moist static energy (MSE) under the weak temperature gradient approximation to tropical dynamics (Sobel et al. 2001).

Two specific feedbacks involving longwave radiation and horizontal advection are commonly emphasized as critical to MJO maintenance and propagation from this view. The first idea is that radiation from high clouds helps energize the MJO. The second idea is that the eastward motion of the MJO is supported through the advection of MSE by its horizontal circulation anomalies. Column MSE budget analysis of the MJO's horizontal structure has supported both of these views, as applied to reanalyses, satellite data, and MJO-permitting global models.

We explore two key hypotheses to this view. The first hypothesis H_1 is that the existence of the MJO depends on a radiative–convective instability—a positive feedback between atmospheric thermal radiation and water vapor anomalies. This is motivated by the fact that longwave heating is a leading-order diabatic balance of the MJO variance column energy budget in MJO-permitting models (Maloney 2009; Andersen and Kuang 2012, hereafter AK12; Kim et al. 2015) and in reanalysis (Kiranmayi and Maloney 2011) and satellite (Ma and Kuang 2011) data. The importance of a longwave feedback mechanism to MJO dynamics is especially motivated by the fact that in MJO-permitting global models, mechanism denial experiments that spatially homogenize longwave heating anomalies can destroy the simulated MJO (Landu and Maloney 2011; Andersen 2012).

The first hypothesis is relevant to an analogy A_1 that has been made between the MJO and convective self-aggregation (spontaneous conglomeration of convective updrafts into large, organized clusters) in the idealized limit of radiative–convective equilibrium (RCE). Here RCE refers to a state in which convective heating balances radiative cooling, neglecting large-scale lateral energy transport into the domain of interest. The analogy between RCE self-aggregation and the MJO is that cloud resolving simulations under RCE can produce MJO-like aggregation and correlations between fields such as MSE, precipitation, surface flux, and longwave radiation anomalies (Bretherton et al. 2005).

It is logical to wonder under H_1 (if A_1 is valid) whether the MJO might cease to exist below a critical temperature threshold. This is based on the fact that the self-aggregation longwave feedback mechanism has the capacity to shut down under a critical temperature threshold somewhere below 20°C (Khairoutdinov and Emanuel 2010; Emanuel et al. 2014; Wing and Emanuel 2014). The existence and magnitude of a critical temperature threshold for RCE self-aggregation and its relevance to MJO dynamics are in debate (Emanuel et al. 2014; Wing and Cronin 2016; Abbot

2014), motivating the need for extreme climate sensitivity testing of MJO dynamics.

Our second hypothesis H_2 is that MJO eddies help it move east by mixing moisture horizontally across sharp meridional gradients. The second hypothesis is motivated by consistent diagnostic phase relationships seen in reanalyses (Benedict and Randall 2007; Kiranmayi and Maloney 2011) and global climate models (Maloney 2009; Maloney et al. 2010; AK12). It is especially supported by MJO phase speed sensitivities found in controlled climate model experiments that have interfered with the horizontal moisture advection process either through the basic state (Maloney et al. 2010) or directly (Pritchard and Bretherton 2014). The idea of H_2 can be encapsulated diffusively in a semiempirical analytic MJO model (Sobel and Maloney 2012). One way to think about this advective propagation mechanism is that the observed MJO is dried on the trailing (western) flank of its moist core by the meridional advection of relatively dry free-tropospheric subtropical air by strong MJO Rossby gyres, and that this western drying is consistent with the MJO's eastward motion if moisture is fundamental to its dynamics.

Whether this process is actually fundamental to the eastward travel of the MJO remains in debate. In their analysis of the reanalysis-derived moisture budget, Hsu and Li (2012) argued for equatorial-wave-driven vertical moisture advection in the PBL as a more prominent controlling factor for eastward propagation, in contrast with the interpretation of Kiranmayi and Maloney (2011), which emphasized free-tropospheric moisture variations. Yang and Ingersoll (2013) argue that the MJO's eastward propagation can be explained by the zonal asymmetry between eastward and westward inertia–gravity waves. Some GCM mechanism denial studies even suggest a resilience of MJO signals to denying the free-tropospheric moisture advection process through basic-state interference and nudging (Hsu et al. 2014).

As a new test of both H_1 and H_2 , and the RCE analogy (i.e., A_1), we use a global climate model with a convincing intrinsic MJO signal and apply it in an idealized setting that has not been previously explored to our knowledge. The first idealization is to vary temperature across an extreme range—from 35° down to 1°C. The expectation from H_1 , if RCE temperature criticality is relevant, is that the MJO should cease to exist below a critical temperature below 20°C. The second idealization is to force the model unusually with globally uniform sea surface temperatures (SSTs) to achieve an exotic basic state that can be exploited to test H_2 . For our model we will show this produces a planet with a background near-tropical meridional MSE gradient that has the opposite sign to what is observed in real-world settings, with an MSE minimum

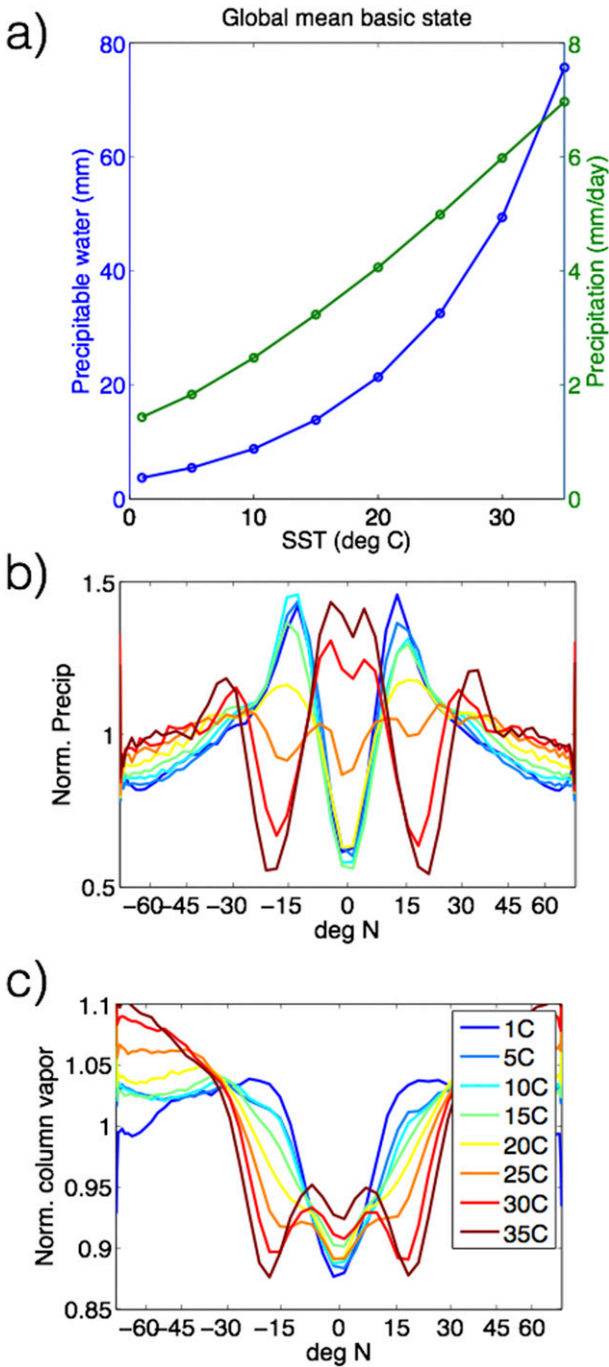


FIG. 1. Longitude- and time-mean state of the simulated climates. (a) Global-mean precipitation and column water vapor across the range of extreme climate variation experiments and (b),(c) their meridional variation (cold-to-warm colors representing coldest-to-warmest SST) normalized by global-mean values in (a).

(rather than a maximum) on the equator. The expectation in this case from H_2 is that an associated reversal of the MSE mixing by MJO-related Rossby gyres should interfere with the ability of the eastward-propagating

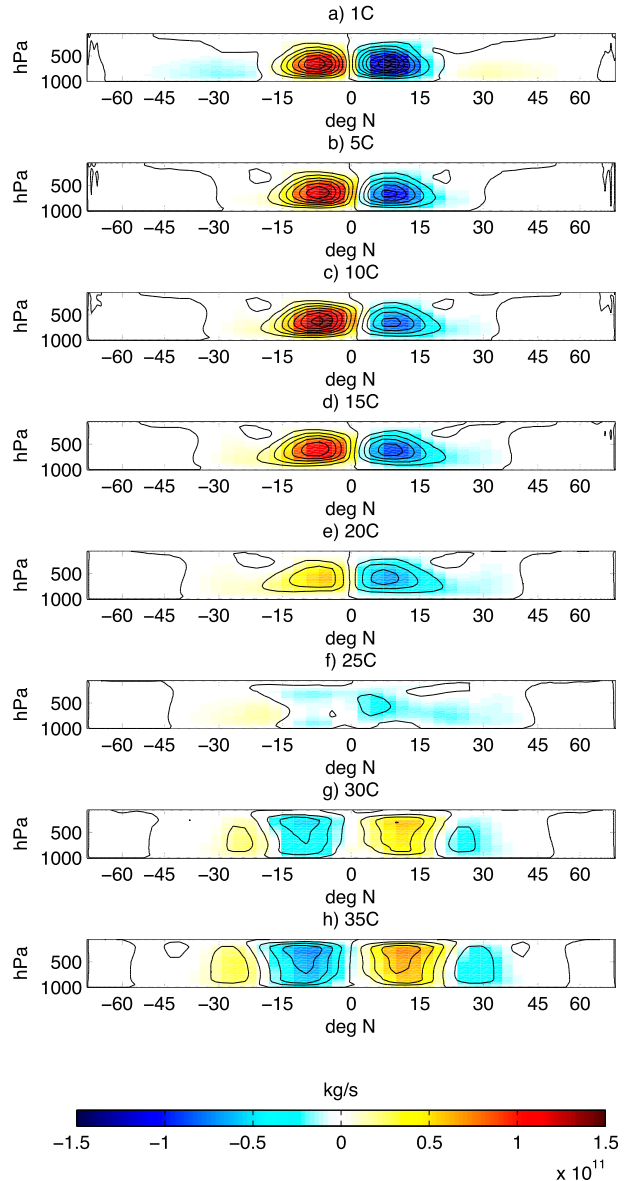


FIG. 2. Time-mean meridional mass circulation for the climates. Contour interval is $2 \times 10^{10} \text{ kg s}^{-1}$ and the zero contour is omitted.

MJO signal to exist at a realistic phase speed. As we will demonstrate, the results on this front are surprising.

2. Methods

We apply the Superparameterized Community Atmosphere Model, version 3.0 (SPCAM3.0), a proven multi-scale global atmospheric model that avoids approximating moist turbulence by explicitly resolving it in $>10,000$ nested cloud system resolving subdomains. SPCAM3.0 is known to produce an unusually realistic MJO signal while making minimal assumptions about deep convection, in both real-geography and idealized settings (Benedict and

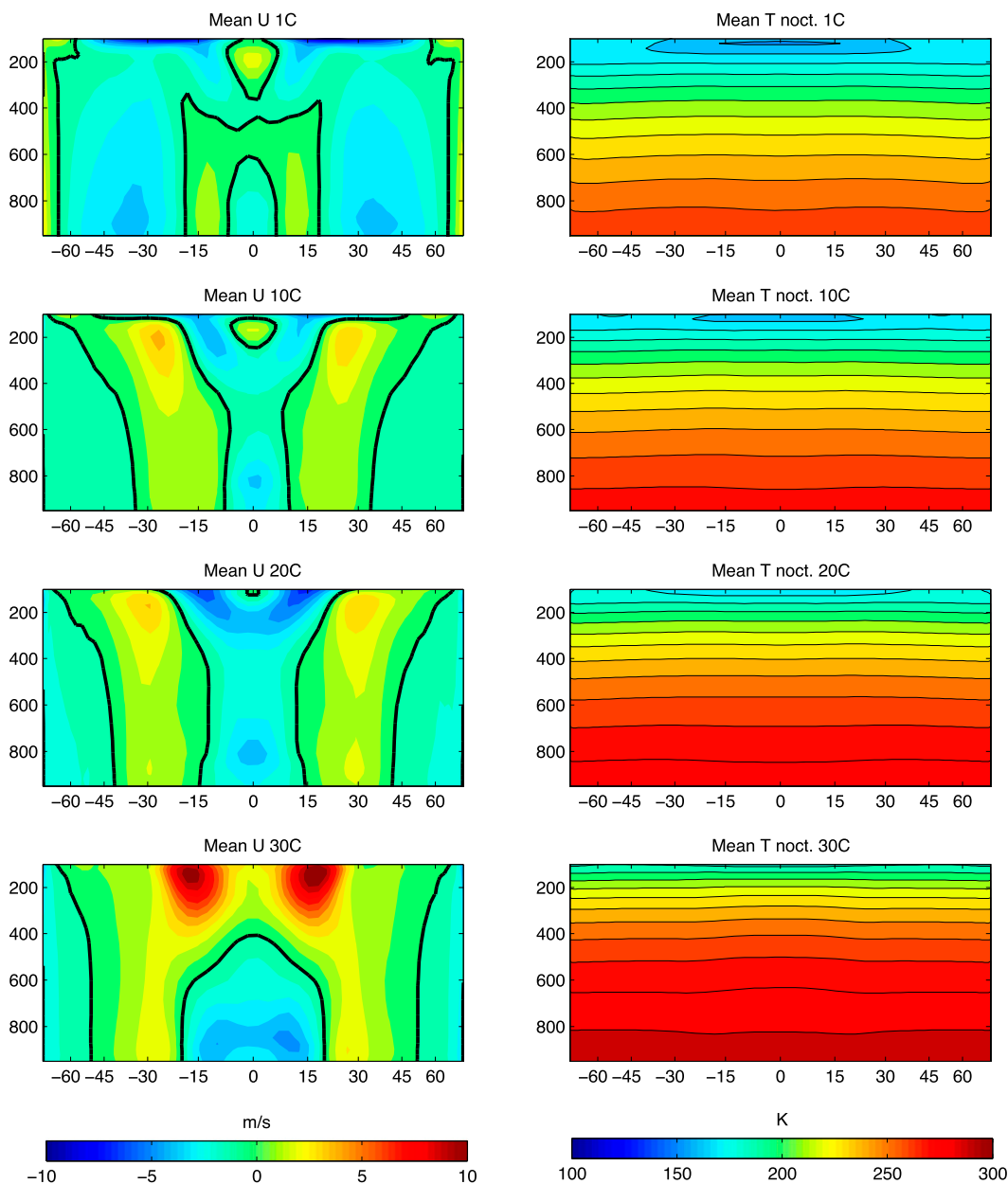


FIG. 3. Time-mean (left) zonal-mean zonal wind and (right) temperature in the simulations.

Randall 2009, 2011; AK12; Arnold et al. 2013; Pritchard et al. 2014; Pritchard and Bretherton 2014). As such it is a useful tool for MJO hypothesis stress testing.

For computational efficiency we use an eightfold accelerated version of SPCAM3.0, using fourfold acceleration from cloud resolving model (CRM) extent reduction (Pritchard et al. 2014), and an additional twofold acceleration using a new time acceleration algorithm (Jones et al. 2015), neither of which significantly impacts SPCAM3.0's intrinsic MJO. This enables a wide ensemble of experiments.

Eight simulations are run with sea surface temperatures spanning an extreme range including many values far below the critical temperature threshold for RCE self-aggregation (1° , 5° , 10° , 15° , 20° , 25° , 30° , and 35°C). The simulations are idealized by removing continents, turning off the sun (perpetual night) and—through homogeneous SSTs—by muting meridional temperature gradients, which deemphasizes extratropical modes of variability and initiates an unusual basic-state climate useful for hypothesis testing. The simulations are analyzed for a 6-yr period following a 2-yr spinup, except for

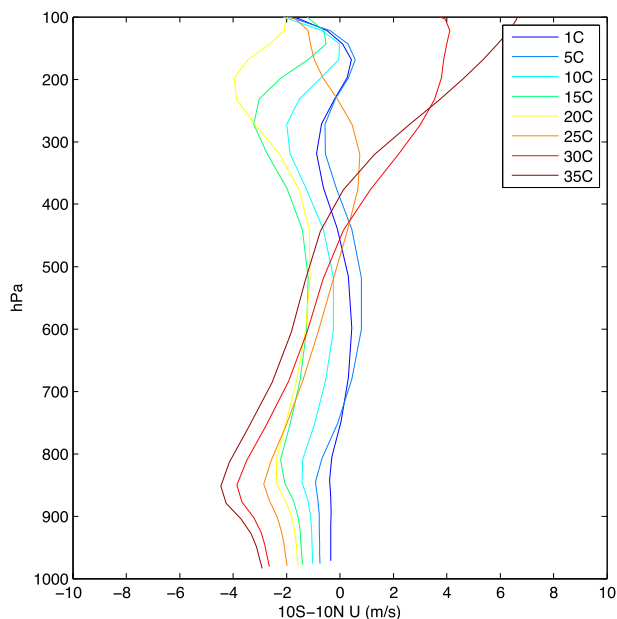


FIG. 4. Time-mean zonal-mean zonal wind on the equator (10°S – 10°N) in the simulations.

the two warmest cases, which are analyzed for a 5-yr period following a 3-month spinup.

3. Results

The basic state in the experiments is summarized in Figs. 1–4. Water vapor and rainfall increase with in-line expectations for extreme climate change (Fig. 1a). An exotic global mass circulation results from using idealized globally homogeneous SSTs in aquaplanet SPCAM3.0 across the range of cold climates examined. For $\text{SST} < 25^{\circ}\text{C}$, each simulated climate exhibits a double-ITCZ-like precipitation structure (Fig. 1b) associated with two circulation cells consisting of ascending, moist air adjacent to the equator near 15°S and 15°N (Fig. 2). For these coldest climates, associated with the double-ITCZ-like circulation anchor is a subsidence structure directly over the equator (Fig. 2), such that relatively dry and MSE-poor tropical air is located on the equator.

For the purpose of testing H_2 , the key property of this idealized circulation is that for $\text{SST} < 25^{\circ}\text{C}$ it happens to reverse the sign of the meridional gradient of basic-state MSE near the equator relative to what is observed in the real climate (Fig. 1b). Following H_2 , this should in turn reverse the ability of MJO eddies to sustain MJO eastward propagation through their advection of basic-state MSE in our coldest simulated climates. That is, for an MJO to exist in these conditions its trailing gyres would have to advect in relatively moist air on the MJO's western flank, which would become inconsistent with

eastward propagation if horizontal advection of moisture is fundamental to it.

As an aside, we note that exotic basic-state general circulations similar to this are not unusual and have been seen by others in GCMs when using globally uniform SSTs (Sumi 1992; Kirtman and Schneider 2000; Chao 2000; Chao and Chen 2004). They are possible because despite the fact that removing sharp extratropical gradients of background MSE drastically damps the overall mass circulation, throttles baroclinic instability, and reduces eddy activity, the existence of rotation alone is nonetheless sufficient to set up a weak basic-state circulation (Chao and Chen 2004). Furthermore, internal variability is such that surface homogenization of SSTs does not ensure perfectly flat isotherms throughout the atmosphere, though it comes close (Fig. 3).

In the coldest climate simulations, the basic-state zonal-mean wind on the equator is very weak and mostly easterly throughout the troposphere but becomes stronger with increasing vertical shear as SST is increased from 1° to 35°C (Fig. 4). Strong vertical shear including super-rotating zonal wind in the upper troposphere is only observed for the warmest cases.

a. Existence of an MJO signal

MJO signal analysis is performed for daily mean anomalies of key state variables (zonal winds, precipitation, and outgoing longwave radiation) averaged within a narrow band directly on the equator, from 5°S to 5°N . We use standard methods (Hayashi 1971) to discriminate eastward- versus westward-propagating tropical signals in observations following the implementation by Wheeler and Kiladis (1999, hereafter WK99), beginning from daily mean anomalies. The only deviation from the procedure of WK99 is that we use a 250-day windowing interval, with overlap of 150 days, in place of the standard nonoverlapping 96-day window. This adjustment accounts for the fact that raw signal analysis reveals the eastward-moving anomaly propagation to be slower than the real-world MJO signal in some of our coldest simulations (Fig. 5).

Figure 6 shows the resulting wavenumber–frequency analysis for the 850-hPa zonal wind U_{850} anomalies. Consistent with the existence of an MJO signal, in each simulated climate a distinct mode of eastward-moving (positive zonal wavenumber) equatorial wind variance is found maximizing at time scales longer than 30 days. In some climates (5° , 20° , 25° , 30° , and 35°C) it is the dominant mode of tropical variability. In other climates (1° , 10° , and 15°C) it is the second most dominant mode, rivaled by a westward-moving intraseasonal mode of equal or greater magnitude. Analysis of raw Hovmöller diagrams of 850 hPa (Fig. 5) confirms that in the cold

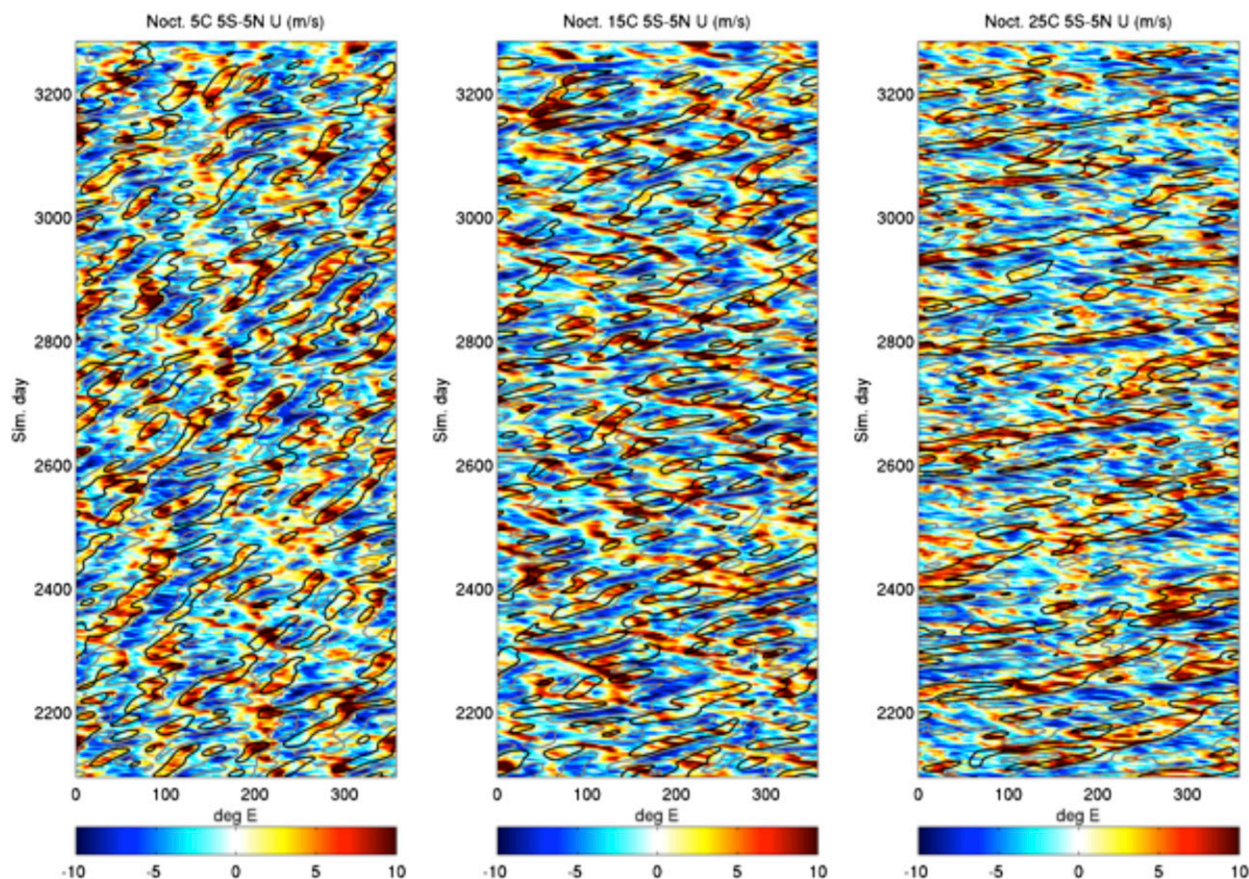


FIG. 5. Time–longitude section showing daily zonal-mean 5°S–5°N 850-hPa zonal wind anomalies with plus/minus (black/gray) one std dev MJO-filtered component superimposed for several cold-climate simulations.

climates these distinct variance maxima are not the result of a standing wave, as can occur using the wavenumber–frequency decomposition methodology (Zhang and Hendon 1997). Rather, unfiltered fields tend to confirm that the model produces a superposition of eastward- and westward-moving modes.

Is the distinct slow eastward-moving mode MJO-like in the cold-climate simulations? This demands multivariate analysis. Figure 7a illustrates conceptually the expected archetypal multivariate phase progression signature of the observed MJO in the time–longitude plane: an eastward-propagating negative (easterly) 850-hPa zonal wind anomaly is followed by three closely linked thermodynamic variations (positive vapor anomaly, positive precipitation anomaly, and negative outgoing longwave radiation anomaly), which are in turned followed by a positive (westerly) 850-hPa anomaly. Figure 7a demonstrates how this archetypal MJO phase relationship can be concisely summarized visually using a smooth color gradation pattern defined across the multiple MJO-modulated state variables involved.

We exploit this new visualization strategy to test whether an MJO-like multivariate phase relationship (Fig. 7a) exists in our simulations in association with the eastward-moving variance mode identified in Fig. 6. Figure 7b visualizes plus/minus one standard deviation of spectrally filtered fields in the hypothesized MJO band (defined initially as zonal wavenumber $k = 1–10$ and time scale $\tau = 20–250$ days in order to encompass both the warm- and cold-climate intraseasonal spectral features in Fig. 6). Consistent with the existence of an MJO-like signal, most of the long-lived zonal wind anomalies that constitute the variance node in Fig. 6 are linked to structures that resemble the MJO’s archetypal phase progression of multiple dynamic and thermodynamic state variables. The MJO-associated thermodynamic and dynamic anomalies propagate eastward at the same speed.

Figures 8 and 9 investigate the three-dimensional dynamic flow structure of the slow eastward-moving signal. Time series of velocity potential and streamfunction on two pressure levels are lag regressed in

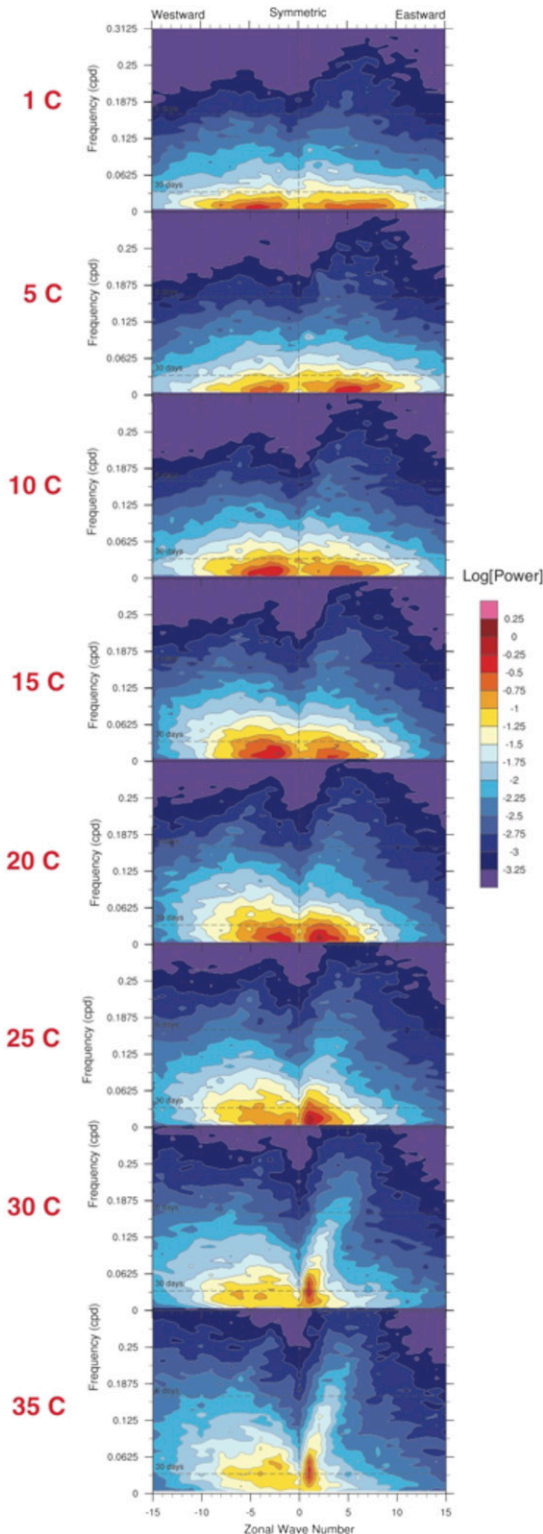


FIG. 6. Equatorial wavenumber–frequency spectra for 5°S–5°N daily mean 850-hPa zonal wind anomalies in all simulations.

horizontal space against a local MJO precipitation index time series (defined as the anomaly of latitudinally averaged precipitation near the equator, filtered spectrally to an MJO band). This process is repeated at many reference longitudes, which leverages zonal symmetry for statistical clarity, following the methods of AK12. To avoid sensitivity to assumed parameters in this method, we vary the latitudinal extent Φ and the spectral bandpass filter settings (maximum zonal wavelength k_{\max} , minimum and maximum time scales τ_1 and τ_2) used to define the precipitation index variable over a 16-member permutation ensemble ($\Phi = 5^\circ, 10^\circ$; $k_{\max} = 10, 15$; $\tau_1 = 20, 40$ days; $\tau_2 = 200, 300$ days) and analyze statistically significant components of the ensemble mean.

The results confirm that the slow eastward-moving mode resembles an MJO with reduced zonal extent. In all climates, the familiar MJO 3D flow structure is clear, consisting of a central velocity potential vertical dipole anomaly in phase with precipitation (Fig. 8) and straddled horizontally by vertically antiphase quadrupole streamfunction anomalies (Fig. 9). The essence of this MJO-like 3D flow pattern survives cooling to temperatures far below 20°–25°C. In the cold climates the zonal scale of the mode is reduced. That the eastward-moving mode is not a Doppler-shifted Rossby wave, which could also have quadrupole dynamic flow anomalies, is confirmed by offline analysis of the mass-weighted barotropic flow, which is insufficient to sustain this (not shown), as also indicated by the mean zonal flow in Fig. 4. Rather, the mode appears to propagate to the east relative to the mean flow as occurs for the MJO.

In summary, because of the above evidence, we conclude that an MJO-like signal exists in each of our uniform-SST aquaplanet simulations, even when $SST < 20^\circ\text{C}$. Figure 10a shows the amplification of the MJO with SST, which scales to first order with mean rainfall across the climates. That is, when normalized by climatological rainfall (Fig. 10b) the relative amplitude of the MJO is remarkably climate invariant.

b. Column moist static energy analysis

The existence of a cold MJO coexisting with reversed basic-state meridional moisture gradients in our simulations for $SST < 25^\circ\text{C}$ is inconsistent with expectations from H_2 , and, thus, could be viewed as challenging moisture mode views of MJO dynamics that emphasize horizontal advection as the key propagation mechanism.

We, therefore, analyze the column MSE budget of the simulated MJO—a diagnostic that has been a cornerstone of the moisture mode interpretation of the MJO (Raymond et al. 2009; Maloney 2009). This is by definition a purely diagnostic framework that highlights correlations between the horizontal structure of the

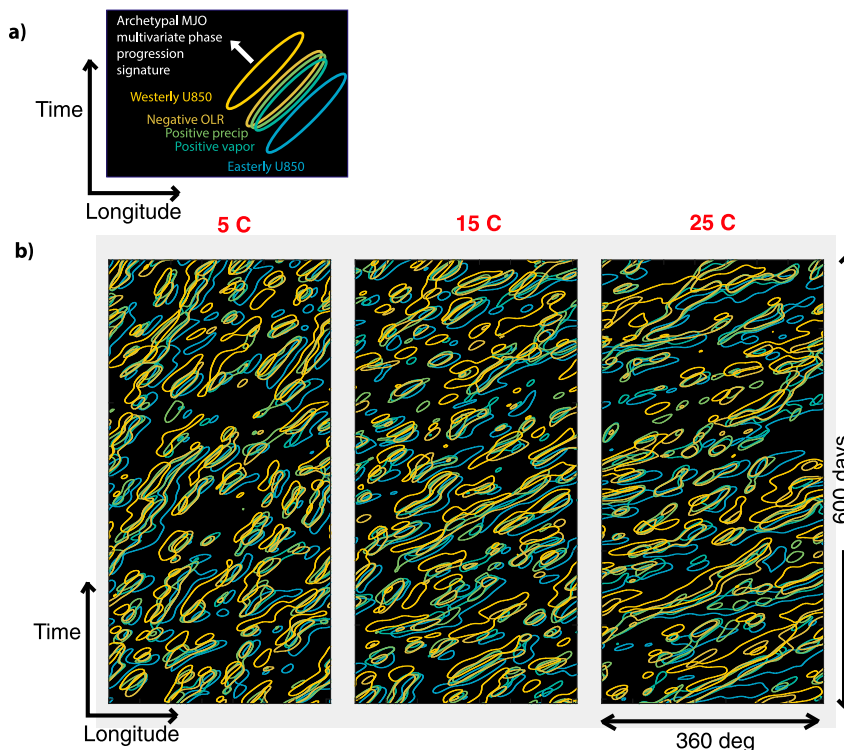


FIG. 7. Multivariate MJO analysis. (a) Demonstration of a new multivariate visualization strategy for compact analysis of the phase progression of an MJO in the time–longitude plane, showing the phase progression of MJO-filtered anomalies in the 5°S – 5°N latitude band, beginning with easterly 850-hPa wind anomalies (minus one std dev), followed by positive vapor and precipitation anomalies (plus one std dev) and negative outgoing longwave radiation anomalies (minus one std dev for vapor and precipitation), and finally westerly 850-hPa wind anomalies (plus one std dev). (b) Application of the method to simulation output, showing an MJO-like phase relationship exists across these variables even in cold climates.

MJO’s MSE anomaly versus terms contributing to its tendency. Such relationships can be viewed as suggestive of the MJO’s fundamental dynamics, though in and of themselves cannot offer causative proof of the processes that control MJO amplitude and phase speed.

To isolate the column MSE budget perturbations associated with the slow eastward-moving rainfall mode, we follow the established methods of AK12. That is, a filtered, latitudinally averaged precipitation index time series is used as a reference against which unfiltered terms in the column MSE budget are lag regressed spatially. By leveraging zonal symmetry, many reference longitudes can be used to enhance statistical significance of the resulting MJO-regression slopes. The regression slopes are in turn scaled by the zonal-mean standard deviation of the MJO index to yield “MJO regressed” horizontal maps of each term in the column MSE budget in physical energy units (see Figs. S1–S4 in the supplemental material). Finally, summary statistics are calculated for each of these terms by projecting their distinct

MJO-regression map onto the map of MJO-regressed MSE, and onto the map of MJO-regressed MSE tendency. Thus, a single compact measure helps discriminate and contrast MSE budget terms contributing to MJO “maintenance” (in phase with MSE) versus “propagation” (in phase with MSE tendency). In practice, the method can be sensitive to several parameter choices such as Φ and the spectral filter settings used to define the MJO index variable (k_{\max} , τ_1 , and τ_2), and the latitudinal extent over which projections are accumulated Φ_p . Therefore, we repeat this calculation 48 times, varying each of these parameters over a 48-member permutation ensemble ($\Phi = 5^{\circ}, 10^{\circ}$; $k_{\max} = 10, 15$; $\tau_1 = 20, 40$ days; $\tau_2 = 200, 300$ days; $\Phi_p = 5^{\circ}, 10^{\circ}, 15^{\circ}$). The resulting MJO MSE budget summary statistics are shown in Fig. 11, and the underlying full MJO-regression maps of column MSE and key tendency contributions are available in Figs. S1–S4 in the supplemental material. We note that the horizontal pattern of precipitation and outgoing longwave radiation anomalies associated with the signal that we have

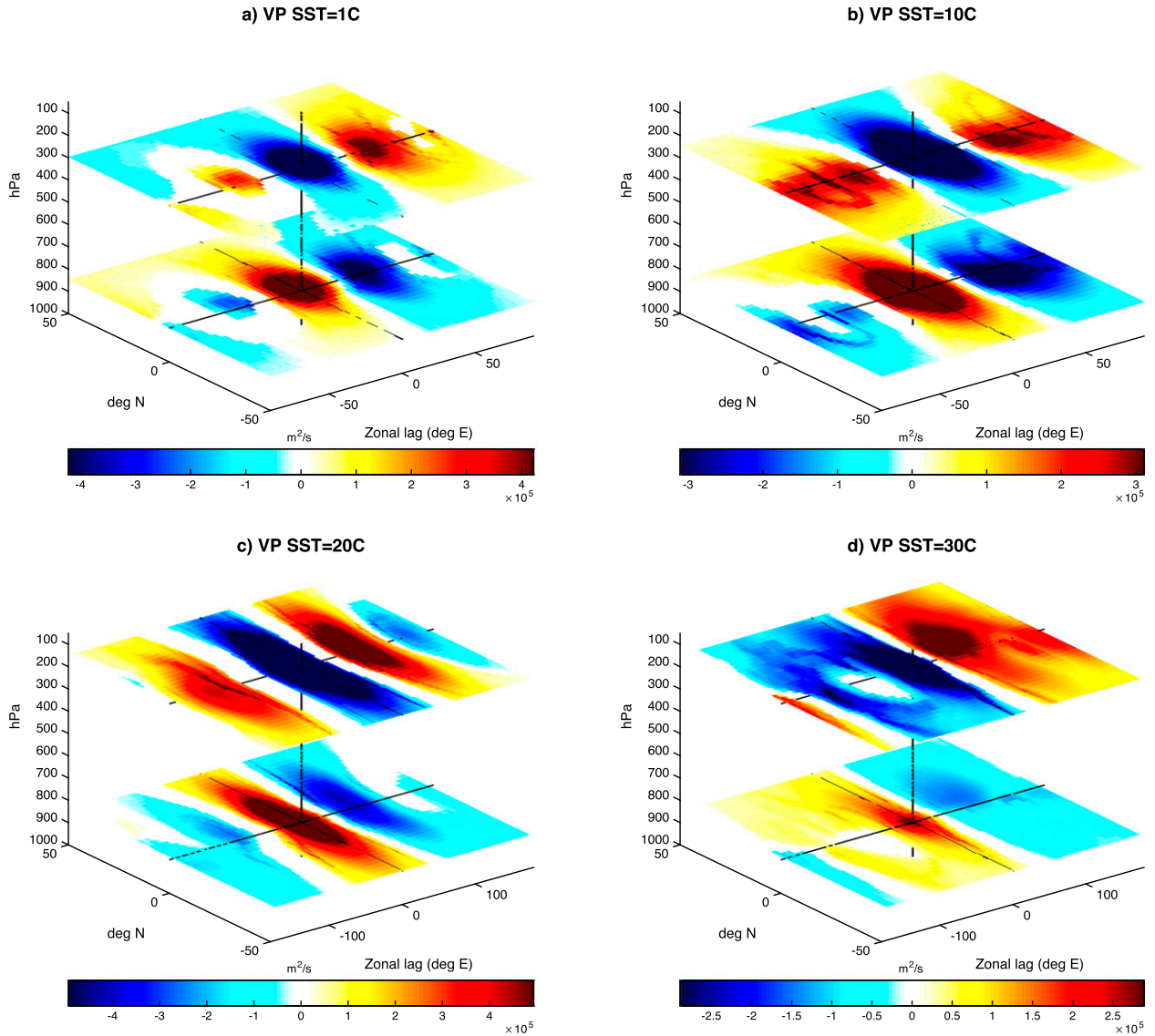


FIG. 8. MJO dynamical structure (velocity potential). Precipitation-regressed velocity potential anomaly for the slow eastward-moving mode for two layers in the lower and upper troposphere, showing a vertically antiphase dipole flow structure reminiscent of the observed MJO mode. Results show the ensemble mean for a 16-member ensemble varying assumed parameters in the filtering/regression method, and are blanked out where indistinguishable from zero at the 95% confidence. The zonal axis range is halved to bring out the smaller horizontal scale of the cold-MJO signal.

isolated closely resemble the column MSE anomaly in Fig. S1 in the supplemental material.

1) PROPAGATION DYNAMICS

Horizontal MSE advection cannot explain the eastward propagation of the MJO-like mode simulated by SPCAM3.0 under constant SST boundary conditions (Fig. 11a). That is, projecting MJO-regressed maps of horizontal MSE advection does not yield leading positive projection values relative to other terms in the MSE budget, as is observed for the MJO in reanalysis and as occurs in real-geography SPCAM3.0 simulations with

warm SSTs. Rather, the propagation projection of horizontal MSE advection is difficult to distinguish from zero within the parameter uncertainty of the regression-projection method. Consistently, the horizontal structure of the MJO-regression map of horizontal column MSE advection does not imply a clear propagating role (see Fig. S4 in the supplemental material). This tends to argue against H_2 that horizontal moisture advection plays an important role in controlling the eastward propagation of the MJO. Rather, the propagation of the MJO in our simulations is balanced primarily through vertical MSE advection. This may suggest that gravity

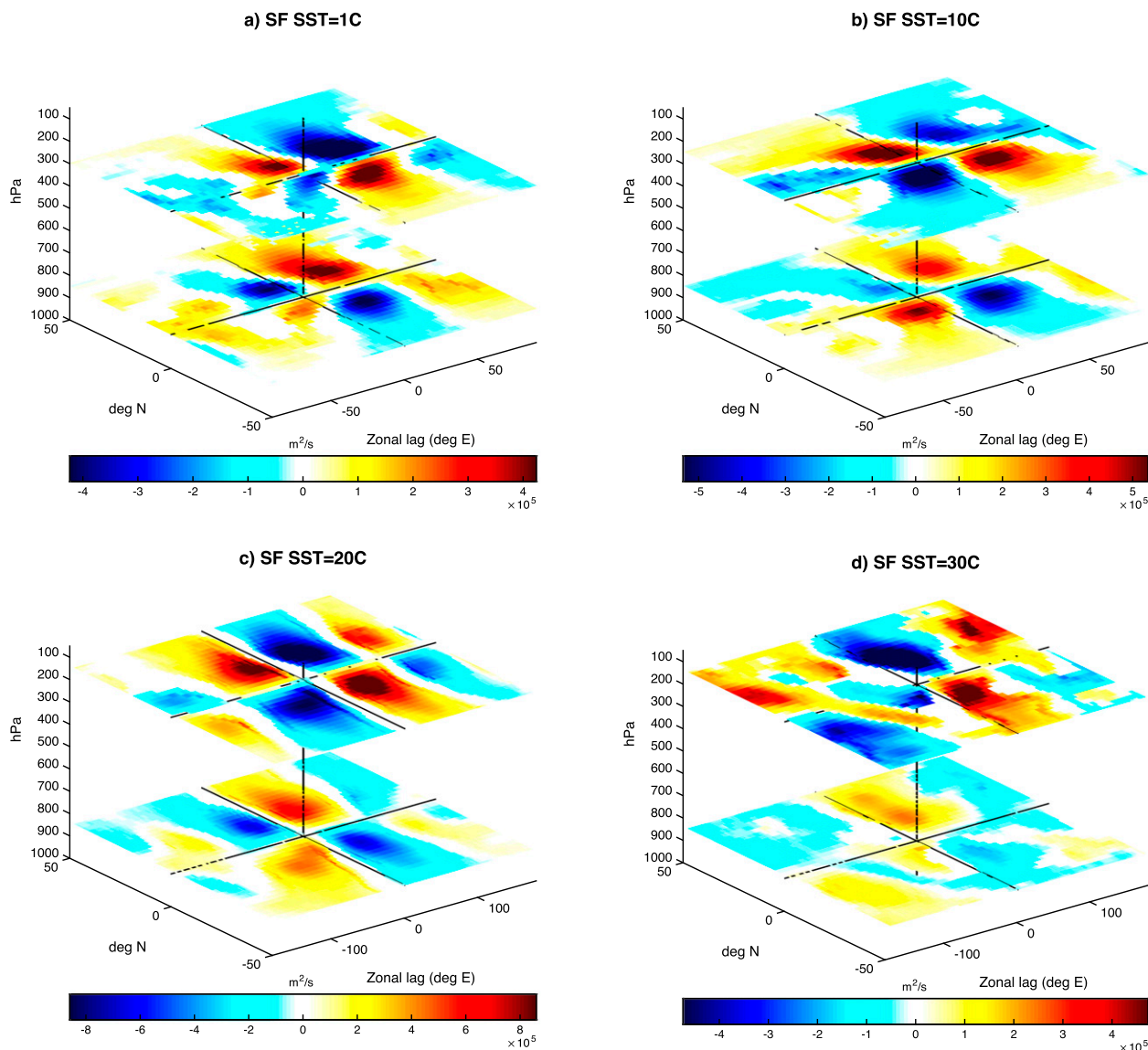


FIG. 9. As in Fig. 8, but for the streamfunction anomaly, showing a vertically antiphase horizontal quadrupole rotational flow anomaly that straddles the central velocity potential dipole, which is also reminiscent of the MJO mode.

acts as a restoring force and leads to the eastward propagation. The possibility of an overarching connection between the cold MJO and these wave classes is explored in further detail in a companion paper.

It is reasonable to consider an alternate interpretation of Fig. 11a—that the modes we have simulated are not in fact MJO-like. This follows if one assumes H_2 is true—that the propagation of the MJO is already known to be due to horizontal moisture advection based on the range of motivating evidence reviewed in the introduction (e.g., Maloney 2009; Maloney et al. 2010; Kiranmayi and Maloney 2011; Sobel and Maloney 2012; AK12; Pritchard and Bretherton 2014). Under this assumption, lack of strong budget projections implicating horizontal

advection, or the predominance of vertical advective terms in our coldest climates, could be viewed as inconsistent with the conclusion that the modes in our simulations are MJO-like. To some extent this is a philosophical question about the extent to which MJO propagation dynamics are well understood, and what it means diagnostically to call a slow eastward-moving intraseasonal mode MJO-like.

Our own view is that the question of why the MJO propagates to the east at its observed rate is not yet fully settled, and that the evidence in Figs. 7–9 is sufficient to claim the modes we have simulated are MJO-like. From this view, if one accepts that the causes of correlations in the MJO's MSE budget are difficult to

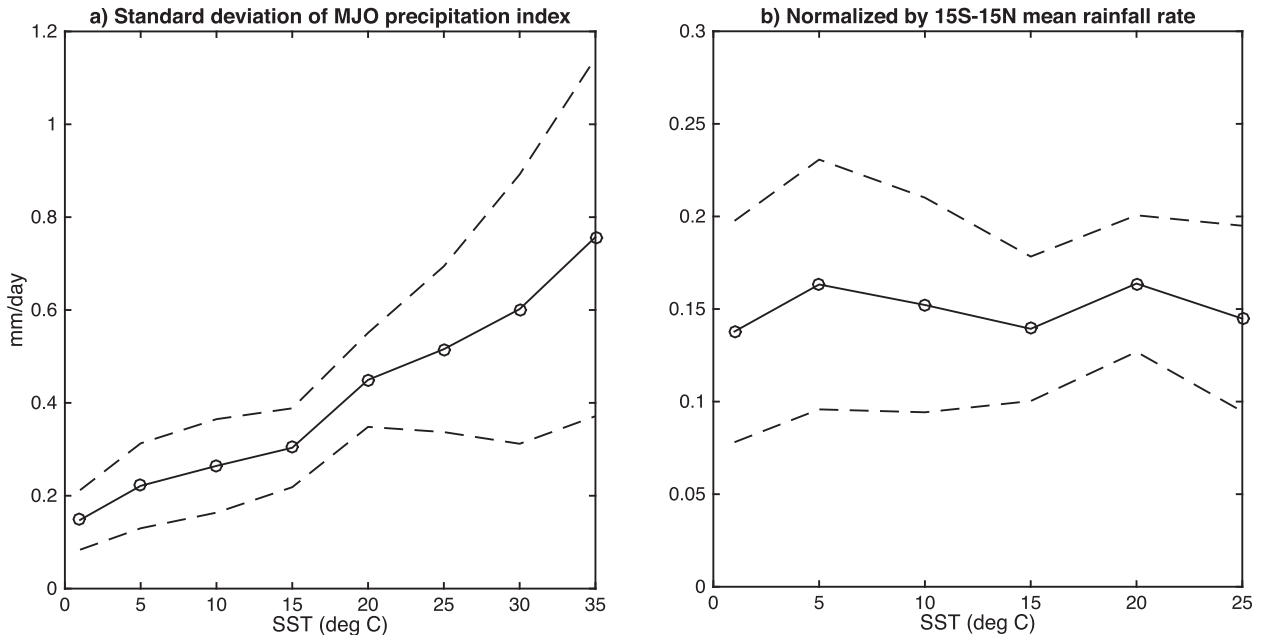


FIG. 10. Amplification of the MJO with SST shown as the (a) zonal-mean temporal std dev of the MJO-filtered rainfall index in each climate, normalized in (b) by the mean tropical rainfall rate. Solid (dashed) lines denote the mean (std dev) from a 16-member ensemble calculation varying the latitudinal extent of the zonal band and the filter settings of the MJO bandpass filter used to define the precipitation index (see text).

fully prove, and if one accepts the possibility that another process may play a controlling role in regulating its eastward propagation, then the existence of an MJO-like signal without a corresponding advective propagation term may be an important, if previously unencountered, counterexample to the advective propagation hypothesis.

2) MAINTENANCE DYNAMICS

Longwave heating anomalies provide the largest and most robustly detectable contribution to MJO MSE maintenance across the entire range of climates (Fig. 11b). For warm climates, this is consistent with ideas from modern moisture mode theory that radiative effects of high clouds and water vapor play an important role in locally energizing the MJO. But for cold climates, this provides a negative answer to our initial question motivated by H_1 about whether the MJO might shut-down due to temperature criticalities of longwave feedbacks of RCE self-aggregation, assuming they are an analogy to the MJO. That is, if SPCAM3.0's MJO is a form of self-aggregation, it is not a temperature-critical one. This is consistent with ideas in other studies that aggregation involving significant longwave effects can occur on small spatial scales even at very cold temperatures under RCE in limited-domain cloud resolving simulations (Abbot 2014) or via shortwave feedbacks in tropical channel simulations (Wing and Cronin 2016).

This is also relevant to questions raised by Emanuel et al. (2014) about the generality of a minimum temperature threshold for aggregation. Our results support the idea that longwave radiative heating anomalies can associate with signals of convective self-aggregation in very cold climates, and demonstrate that this can occur on global scales in the form of cold-MJO-like signals.

Our results suggest that physics other than the efficiency of vertical MSE advection may play a role in orchestrating the amplification of the MJO with SST warming, an idea that is further explored in a companion paper. The climate sensitivity of the MJO in the vicinity of current temperatures has been linked to systematic changes in the efficiency of vertical MSE advection in its maintenance dynamics (Arnold et al. 2013). Consistent with an extension of this idea across a broader SST range, the efficiency of this damping term is strongly reduced as SST is warmed from 1° to 30°C (Fig. 11b). However, one difference in our findings is that we do not detect a transition from a dissipative to an amplifying role (sign flip) for the vertical advection term in the 25°–35°C SST range, indicating that this aspect of the MJO response may be basic-state dependent. We also find an interesting counterexample to this mechanism in that the efficiency of the vertical advection term is not detectably sensitive to increasing SST from 30° to 35°C in our simulations, despite MJO amplification in this climate regime (Fig. 10).

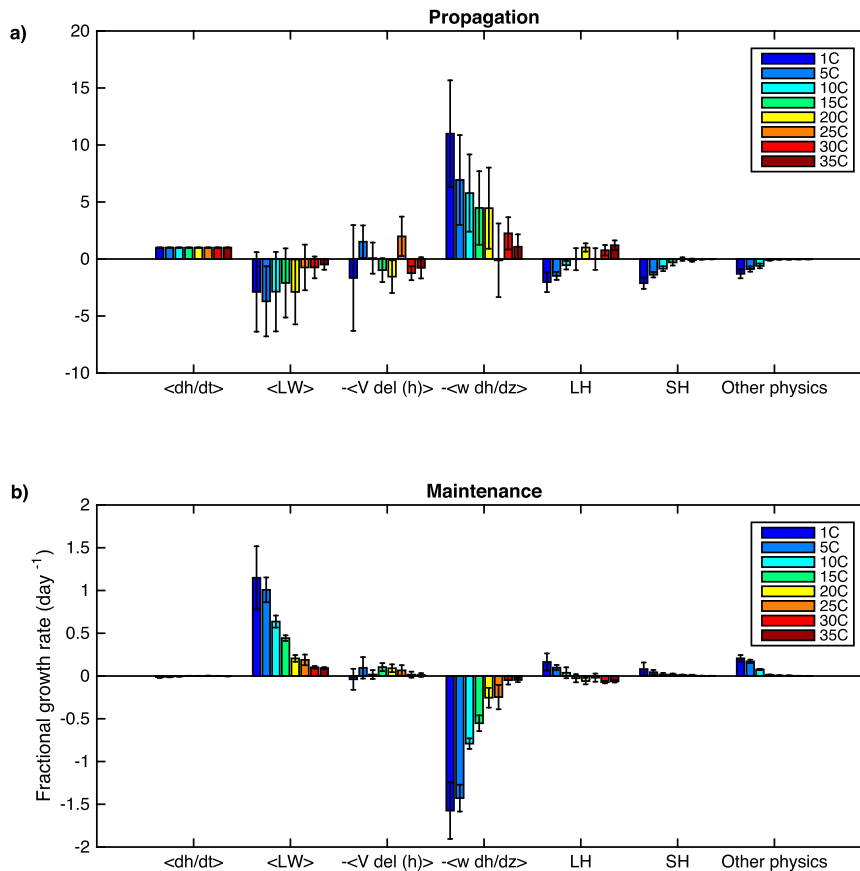


FIG. 11. Summary statistics describing the column MSE h budget associated with the MJO in each climate. (a) Projection of maps of MJO-regressed terms in the column MSE budget onto the map of MJO-regressed column MSE tendency (dh/dt), to yield the propagation summary diagnostic. (b) As in (a), but for the maintenance summary diagnostic by projecting onto MSE tendency. Bar heights and std devs denote the ensemble mean and std dev from a 48-member ensemble of calculations varying assumed parameters in the regression–projection method (see text and Figs. S3–S6 in the supplemental material for further details). The term “other physics” denotes the residual between the model’s total physics package diabatic tendency and the sum of individually tracked contributions from longwave (LW), latent (LH), and sensible (SH) heating.

4. Conclusions

We have performed idealized experiments using a novel global climate model (SPCAM3.0) that produces a realistic MJO signal while making minimal assumptions about how moist convection interacts with large-scale dynamics. We have used this model to test two hypotheses (H_1 and H_2) motivated by a modern view of the “moisture mode” theory of the MJO and an analogy (A_1) that the MJO is an analog to temperature-critical RCE self-aggregation. Inconsistent with A_1 , we have found that the MJO does not shut down even for very cold climates down to 1°C. Evidence of a cold-MJO signal exists from a variety of diagnostic vantage points. Apparently the intrinsic MJO signal in SPCAM3.0 is a surprisingly resilient mode that can survive extreme

cooling of the climate. Inconsistent with H_2 , the MJO in SPCAM3.0 can also survive a reversal of near-equatorial meridional MSE gradients that occurs in our coldest simulations due to exotic basic-state responses to homogeneous SSTs.

The existence of a cold MJO in our simulations might raise some troubling concerns about the validity of a moisture mode interpretation, including ideas that the MJO is propagated by horizontal moisture advection or critically dependent on SST > 25°C. The fact that the cold MJO can occur even in a weakly sheared easterly basic state is also hard to reconcile with ideas related to vertical shearing of its longwave heating anomaly as an MJO propagation mechanism. Resilience of familiar phase relationships among terms in the MJO-column MSE budget in our simulations (leading longwave

maintenance and vertical MSE advective dissipation) could indicate some broader cause requires such correlations to exist.

Convective self-aggregation arguments could nonetheless be invoked to explain the MJO signals in our simulations via dynamics that are unfamiliar insofar as they would rely on positive longwave feedback even at cold SST and could not rely on horizontal MSE advection as the primary propagation mechanism. The fact that longwave heating anomalies are in phase with MSE anomalies is consistent with H_1 and could explain the maintenance of the MJO through aggregation at low effective gross moist stability. A horizontal phase offset in vertical motion and balanced equatorial beta-plane dynamics could then require moist anomalies to move east or west independent of horizontal advection (C. Bretherton 2015, personal communication). Detailed analysis of the initial development of moist anomalies might help elucidate if such dynamics help cause a cold MJO in a horizontally uniform SST setting.

An alternate hypothesis is that dynamics more fundamentally tied to high-frequency equatorial waves and scale interactions provide an overarching control on the MJO across our simulations, consistent with the gravity wave-like signatures in its composite MSE balance in Fig. 11a. This is also consistent with the fact that the MJO can be simulated without interactive radiation at constant SST in global models with explicit convection (Grabowski 2001) and without meridional moisture gradients in conventionally parameterized aquaplanet experiments (Hsu et al. 2014). In a companion paper, we test predictions from the recent theory of Yang and Ingersoll (2013, 2014) and find they exhibit skill in quantitatively predicting both the zonal enlargement and speedup of the MJO seen in our simulations, consistent with their idea that the MJO may be a large-scale envelope of high-frequency small-scale tropical waves.

Meanwhile, this simulation suite provides a useful test bed for modern theories of the MJO since it quantifies MJO amplification, enlargement, and speedup across the 1°–35°C climate regime, in a relatively simple basic state. It would be worth testing predictions from more MJO theories against these simulation results, and testing their resilience across multiple MJO-permitting global climate models.

Acknowledgments. Funding for this work was provided by the U.S. Department of Energy under DE-SC0012152 and DE-SC0012548 and by the National Science Foundation (NSF) under AGS-1419518. Da Yang is supported by a fellowship from the Miller Institute for Basic Research in Science at UC Berkeley. Computational resources were provided by the Extreme

Science and Engineering Discovery Environment, which is supported by NSF Grant OCI-1053575, under Allocation TG-ATM120034.

REFERENCES

- Abbot, D. S., 2014: Resolved snowball earth clouds. *J. Climate*, **27**, 4391–4402, doi:[10.1175/JCLI-D-13-00738.1](https://doi.org/10.1175/JCLI-D-13-00738.1).
- Andersen, J. A., 2012: Investigations of the convectively coupled equatorial waves and the Madden–Julian oscillation. Ph.D. dissertation, Department of Physics, Harvard University, 270 pp.
- , and Z. Kuang, 2012: Moist static energy budget of MJO-like disturbances in the atmosphere of a zonally symmetric aquaplanet. *J. Climate*, **25**, 2782–2804, doi:[10.1175/JCLI-D-11-00168.1](https://doi.org/10.1175/JCLI-D-11-00168.1).
- Arnold, N. P., Z. Kuang, and E. Tziperman, 2013: Enhanced MJO-like variability at high SST. *J. Climate*, **26**, 988–1001, doi:[10.1175/JCLI-D-12-00272.1](https://doi.org/10.1175/JCLI-D-12-00272.1).
- Benedict, J. J., and D. A. Randall, 2007: Observed characteristics of the MJO relative to maximum rainfall. *J. Atmos. Sci.*, **64**, 2332–2354, doi:[10.1175/JAS3968.1](https://doi.org/10.1175/JAS3968.1).
- , and —, 2009: Structure of the Madden–Julian oscillation in the Superparameterized CAM. *J. Atmos. Sci.*, **66**, 3277–3296, doi:[10.1175/2009JAS3030.1](https://doi.org/10.1175/2009JAS3030.1).
- , and —, 2011: Impacts of idealized air–sea coupling on Madden–Julian oscillation structure in the Superparameterized CAM. *J. Atmos. Sci.*, **68**, 1990–2008, doi:[10.1175/JAS-D-11-04.1](https://doi.org/10.1175/JAS-D-11-04.1).
- Bretherton, C. S., P. N. Blossey, and M. Khairoutdinov, 2005: An energy-balance analysis of deep convective self-aggregation above uniform SST. *J. Atmos. Sci.*, **62**, 4273–4292, doi:[10.1175/JAS3614.1](https://doi.org/10.1175/JAS3614.1).
- Chao, W. C., 2000: Multiple quasi equilibria of the ITCZ and the origin of monsoon onset. *J. Atmos. Sci.*, **57**, 641–652, doi:[10.1175/1520-0469\(2000\)057<0641:MQEOTI>2.0.CO;2](https://doi.org/10.1175/1520-0469(2000)057<0641:MQEOTI>2.0.CO;2).
- , and B. Chen, 2004: Single and double ITCZ in an aqua-planet model with constant sea surface temperature and solar angle. *Climate Dyn.*, **22**, 447–459, doi:[10.1007/s00382-003-0387-4](https://doi.org/10.1007/s00382-003-0387-4).
- Emanuel, K., A. A. Wing, and E. M. Vincent, 2014: Radiative-convective instability. *J. Adv. Model. Earth Syst.*, **6**, 75–90, doi:[10.1002/2013MS000270](https://doi.org/10.1002/2013MS000270).
- Grabowski, W. W., 2001: Coupling cloud processes with the large-scale dynamics using the Cloud-Resolving Convection Parameterization (CRCP). *J. Atmos. Sci.*, **58**, 978–997, doi:[10.1175/1520-0469\(2001\)058<0978:CCPWTLL>2.0.CO;2](https://doi.org/10.1175/1520-0469(2001)058<0978:CCPWTLL>2.0.CO;2).
- , and P. K. Smolarkiewicz, 1999: A Cloud Resolving Convective Parameterization for modeling the tropical convective atmosphere. *Physica D*, **133**, 171–178, doi:[10.1016/S0167-2789\(99\)00104-9](https://doi.org/10.1016/S0167-2789(99)00104-9).
- Hayashi, Y., 1971: A generalized method of resolving disturbances into progressive and retrogressive waves by space Fourier and time cross-spectral analyses. *J. Meteor. Soc. Japan*, **49**, 125–128.
- Hsu, P.-C., and T. Li, 2012: Role of the boundary layer moisture asymmetry in causing the eastward propagation of the Madden–Julian oscillation. *J. Climate*, **25**, 4914–4931, doi:[10.1175/JCLI-D-11-00310.1](https://doi.org/10.1175/JCLI-D-11-00310.1).
- , —, and H. Murakami, 2014: Moisture asymmetry and MJO eastward propagation in an aqua-planet general circulation model. *J. Climate*, **27**, 8747–8760, doi:[10.1175/JCLI-D-14-00148.1](https://doi.org/10.1175/JCLI-D-14-00148.1).

- Jones, C. R., C. S. Bretherton, and M. S. Pritchard, 2015: Mean-state acceleration of cloud-resolving models and large eddy simulations. *J. Adv. Model. Earth Syst.*, **7**, 1643–1660, doi:10.1002/2015MS000488.
- Khairoutdinov, M., and K. Emanuel, 2010: Aggregated convection and the regulation of tropical climate. *29th Conf. on Hurricanes and Tropical Meteorology*, Tucson, AZ, Amer. Meteor. Soc., P2.69. [Available online at https://ams.confex.com/ams/29Hurricanes/techprogram/paper_168418.htm.]
- , D. Randall, and C. DeMott, 2005: Simulations of the atmospheric general circulation using a cloud-resolving model as a superparameterization of physical processes. *J. Atmos. Sci.*, **62**, 2136–2154, doi:10.1175/JAS3453.1.
- , C. DeMott, and D. Randall, 2008: Evaluation of the simulated interannual and subseasonal variability in an AMIP-style simulation using the CSU multiscale modeling framework. *J. Climate*, **21**, 413–431, doi:10.1175/2007JCLI1630.1.
- Kim, D., M.-S. Ahn, I.-S. Kang, and A. D. Del Genio, 2015: Role of longwave cloud–radiation feedback in the simulation of the Madden–Julian oscillation. *J. Climate*, **28**, 6979–6994, doi:10.1175/JCLI-D-14-00767.1.
- Kiranmayi, L., and E. D. Maloney, 2011: Intraseasonal moist static energy budget in reanalysis data. *J. Geophys. Res.*, **116**, D21117, doi:10.1029/2011JD016031.
- Kirtman, B. P., and E. K. Schneider, 2000: A spontaneously generated tropical atmospheric general circulation. *J. Atmos. Sci.*, **57**, 2080–2093, doi:10.1175/1520-0469(2000)057<2080:ASGTAG>2.0.CO;2.
- Landu, K., and E. D. Maloney, 2011: Effect of SST distribution and radiative feedbacks on the simulation of intraseasonal variability in an aquaplanet GCM. *J. Meteor. Soc. Japan*, **89**, 195–210, doi:10.2151/jmsj.2011-302.
- Ma, D., and Z. Kuang, 2011: Modulation of radiative heating by the Madden–Julian oscillation and convectively coupled Kelvin waves as observed by *CloudSat*. *Geophys. Res. Lett.*, **38**, L21813, doi:10.1029/2011GL049734.
- Majda, A. J., and S. N. Stechmann, 2009: The skeleton of tropical intraseasonal oscillations. *Proc. Natl. Acad. Sci. USA*, **106**, 8417–8422, doi:10.1073/pnas.0903367106.
- Maloney, E. D., 2009: The moist static energy budget of a composite tropical intraseasonal oscillation in a climate model. *J. Climate*, **22**, 711–729, doi:10.1175/2008JCLI2542.1.
- , A. H. Sobel, and W. M. Hannah, 2010: Intraseasonal variability in an aquaplanet general circulation model. *J. Adv. Model. Earth Syst.*, **2** (5), doi:10.3894/JAMES.2010.2.5.
- Pritchard, M. S., and C. S. Bretherton, 2014: Causal evidence that rotational moisture advection is critical to the superparameterized Madden–Julian oscillation. *J. Atmos. Sci.*, **71**, 800–815, doi:10.1175/JAS-D-13-0119.1.
- , —, and C. A. DeMott, 2014: Restricting 32–128 km horizontal scales hardly affects the MJO in the Superparameterized Community Atmosphere Model v.3.0 but the number of cloud-resolving grid columns constrains vertical mixing. *J. Adv. Model. Earth Syst.*, **6**, 723–739, doi:10.1002/2014MS000340.
- Randall, D., M. Khairoutdinov, A. Arakawa, and W. Grabowski, 2003: Breaking the cloud parameterization deadlock. *Bull. Amer. Meteor. Soc.*, **84**, 1547–1562, doi:10.1175/BAMS-84-11-1547.
- Raymond, D. J., and Ž. Fuchs, 2009: Moisture modes and the Madden–Julian oscillation. *J. Climate*, **22**, 3031–3046, doi:10.1175/2008JCLI2739.1.
- , S. L. Sessions, A. H. Sobel, and Ž. Fuchs, 2009: The mechanics of gross moist stability. *J. Adv. Model. Earth Syst.*, **1** (9), doi:10.3894/JAMES.2009.1.9.
- Sobel, A., and E. Maloney, 2012: An idealized semi-empirical framework for modeling the Madden–Julian oscillation. *J. Atmos. Sci.*, **69**, 1691–1705, doi:10.1175/JAS-D-11-0118.1.
- , J. Nilsson, and L. M. Polvani, 2001: The weak temperature gradient approximation and balanced tropical moisture waves. *J. Atmos. Sci.*, **58**, 3650–3665, doi:10.1175/1520-0469(2001)058<3650:TWTGAA>2.0.CO;2.
- Sumi, A., 1992: Pattern formation of convective activity over the aqua-planet with globally uniform sea surface temperature (SST). *J. Meteor. Soc. Japan*, **70**, 855–876.
- Wheeler, M., and G. N. Kiladis, 1999: Convectively coupled equatorial waves: Analysis of clouds and temperature in the wavenumber–frequency domain. *J. Atmos. Sci.*, **56**, 374–399, doi:10.1175/1520-0469(1999)056<0374:CCEWAO>2.0.CO;2.
- Wing, A. A., and K. A. Emanuel, 2014: Physical mechanisms controlling self-aggregation of convection in idealized numerical modeling simulations. *J. Adv. Model. Earth Syst.*, **6**, 59–74, doi:10.1002/2013MS000269.
- , and T. W. Cronin, 2016: Self-aggregation of convection in long channel geometry. *Quart. J. Roy. Meteor. Soc.*, **142**, 1–15, doi:10.1002/qj.2628.
- Yang, D., and A. P. Ingersoll, 2013: Triggered convection, gravity waves, and the MJO: A shallow-water model. *J. Atmos. Sci.*, **70**, 2476–2486, doi:10.1175/JAS-D-12-0255.1.
- , and —, 2014: A theory of the MJO horizontal scale. *Geophys. Res. Lett.*, **41**, 1059–1064, doi:10.1002/2013GL058542.
- Zhang, C., 2005: Madden–Julian oscillation. *Rev. Geophys.*, **43**, RG2003, doi:10.1029/2004RG000158.
- , and H. H. Hendon, 1997: Propagating and standing components of the intraseasonal oscillation in tropical convection. *J. Atmos. Sci.*, **54**, 741–752, doi:10.1175/1520-0469(1997)054<0741:PASCOT>2.0.CO;2.